Strontium-90 in Surface Air and the Stratosphere: Some Interpretations of the 1963–75 Data

D. O. STALEY

Department of Atmospheric Sciences, The University of Arizona, Tucson 85721

(Manuscript received 14 September 1981, in final form 11 March 1982)

ABSTRACT

Stratospheric inventories of Sr-90 over the period 1963–75 yield $T_{1/2*}$ = 6–7 months for the inventory difference between Northern and Southern Hemispheres, $T_{1/2N}$ = 9–10 months for the decay of the Northern Hemispheric inventory by transfer to the troposphere and Southern Hemisphere, $T_{1/2T}$ = 10–11 months for the decay of the total stratospheric inventory, and $T_{1/2E}$ = 2.5–3.5 years for the decay of the Northern Hemispheric inventory by transfer to the Southern Hemisphere alone.

Mean monthly concentrations of Sr-90 in surface air along the 80th meridian are computed for the years 1963–75 and presented in time-latitude cross sections. The spring maximum in the Northern Hemisphere appears first at the lowest latitude (Miraflores-Balboa, 9°N) for which data are available. The reason for this appears to be seasonal precipitation scavenging associated with seasonal migrations of the equatorial trough (ITCZ). In the tropics and subtropics, where precipitation rate shows large seasonal variations, the Sr-90 concentration in surface air is related to precipitation rate in a manner qualitatively similar to that predicted by a simple theory based on precipitation scavenging and a constant source.

The standard error of the data is small in both hemispheres and similar to the pattern of Sr-90 concentration. The standard error is inversely related to the precipitation rate. However, longitudinal comparisons are inadequate in the Southern Hemisphere to confirm that the Sr-90 concentrations of the 80th meridian network are representative.

1. Introduction

As a tracer of global air motion, fission-product radioactivity offers some important advantages over trace gases such as ozone and water vapor, thermodynamic entities such as potential and equivalent potential temperature, and thermodynamical-dynamical quantities such as potential vorticity. All of the latter tracers are subject to one or more of radiative, photochemical, chemical and dynamical processes. The advantages of fission-product radioactivity include the availability of a great variety of radioisotopes suitable for tracing motions for a few days (I-131, 8.04 days half-life) to many years (Sr-90, 28.82 years; Cs-137, 30.17 years), and an instantaneous point source (or, if not quite a point source, at least a source along a short vertical line). Activity ratios and special tracers such as the neutron activation products W-185 (78.8 days), Rh-102 (210 days) and Cd-109 (410 days) have been used to distinguish between radioactivity produced by nuclear weapons tests made at different times and altitudes.

Disadvantages include the fact that atmospheric injections of radioactivity are largely gratuitous for meteorologists; time and location of injection could usually have been better chosen for the purpose of meteorological experimentation. Other disadvantages include poor data coverage and uncertain settling and removal physics.

During the mid-1950s, the stratospheric inventory of long-lived fission products built up as a result of weapons testing by the United Kingdom, the USSR and the United States. After a period of decreased testing in 1960 and early 1961, testing of large-yield weapons, including a superbomb of 58 megatons, resumed in late 1961 by the USSR and continued into 1962 by the USSR and the United States.

From the mid-1950s onward, fission-product radioactivity has been measured, among other places, in soils, drinking water, food, milk, the skeleton, precipitation, the stratosphere, the troposphere and in surface air. The most extensive and long-enduring surface-air network in the Western Hemisphere was set up by the Naval Research Laboratory along the 80th meridian (West) of both hemispheres in 1957. It was soon apparent (Lockhart *et al.*, 1960) that a pronounced spring maximum of fission-product radioactivity occurred every year in surface air, with maximum amplitude in middle latitudes. Gustafson (1961) presented Cs-137 concentrations in surface air at Argonne National Laboratory for the years 1953–60. Despite nuclear testing at irregular intervals that built up the stratospheric reservoir and gave temporary fluctuations to activity in the troposphere (~20 days half-residence time), a spring maximum of Cs-137 was not only obvious each year, but also exceeded any other maxima that occurred in the

0022-4928/82/071571-20$09.00

same year. A fall minimum was equally obvious each year. Activity at the time of the spring maximum averaged seven times larger than the fall minimum for the years 1953–60. Averaging of these data by Staley (1962) showed the spring maximum occurring on 1 May and the fall minimum on 1 November.

Another important aspect of fission-product radioactivity which was of early concern was its residence time in the stratosphere. Libby (1956) proposed a half-residence time of ~10 years, which would reduce the biological hazard from Sr-90 fallout. This number was disputed by Machta (1957) and Martell (1959), and eventually a value of the order of 1 year was recognized as being more realistic for the stratosphere as a whole.

The stratospheric residence time is related to radioactivity transport within the stratosphere and to mass exchange across the tropopause. This mass exchange, in turn, affects the levels of radioactivity observed in surface air. Reed and Sanders (1953) and Reed (1955) showed by case studies the probability of significant lower-stratospheric mass entering the upper troposphere below the jet stream just to the west of extratropical cyclones. Staley (1960), in another case study, traced air trajectories downward and southward from the lower stratosphere to the lower troposphere, where it was characterized by large stability, large potential vorticity, and very low relative humidity. He estimated that such mass intrusions were quantitatively significant and that recent stratospheric air is cast off from the parent cyclone and does not soon return to the stratosphere, thereby allowing sufficient opportunity for removal from the troposphere. It remained actually to measure relatively high fission-product radioactivity in the descending air within stable baroclinic zones associated with intense cyclogenesis. Staley (1962) measured fission-product gross beta activity below, within and above several stable baroclinic zones over Tucson. The zones were associated with cyclogenesis, and trajectories, where data allowed tracing them back, mostly confirmed a recent stratospheric origin. Reiter (1963) and Danielsen (1964) have added to the measurements confirming the association of cyclogenesis with transport of radioactivity out of the stratosphere in temperate and higher latitudes.

If mass transport out of the stratosphere is dominated by that associated with extratropical cyclones and if tropospheric half-residence time is short ($\leqslant$3 weeks), then maximum concentration in surface air and maximum deposition on the earth's surface should be found well outside the tropics. This is indeed the case. Hardy *et al.* (1968), using soil sampled since 1955 at sites around the world, show maxima of deposited Sr-90 at 45°N and 40°S, with minima near the equator and at the poles. As noted above, Lockhart *et al.* (1960) found maximum surface-air concentrations away from the equator.

How is the spring maximum to be explained? Baroclinic instability and intense extratropical cyclogenesis are seasonal, and maximum mass exchange across the tropopause might be expected in winter and minimum in summer. However, the existence of a spring maximum and a fall minimum in surface air shows that more is occurring than a simple seasonal variation of mass exchange. Two other influences have been noted: seasonal fluctuations of stratospheric mass, and seasonal variations of tracer transport within the stratosphere.

The first of these influences was suggested by Staley (1962), who showed that the decrease of stratospheric mass from January to July could be very large. For example, from January to July 1957 at Greensboro (36°N), tropopause pressure decreased from 224 to 131 mb, corresponding to a 42% decrease of stratospheric mass. For the same period, tropopause pressure at Swan Island (17°N) increased from 94 to 105 mb, for a 10% increase of stratospheric mass. Measurements show that the concentration of radioactivity increases rapidly upward above the tropopause, which may be regarded as the top of a global boundary layer within which air is mixed rapidly and particulates are rapidly scavenged by precipitation. Whatever the radiative and dynamical reasons for seasonal changes of tropopause height, it is clear that in spring, as the tropopause moves upward into regions of higher radioactivity concentration, lower stratospheric air which was previously protected from active vertical mixing finds itself in the troposphere and subject to active vertical mixing. In the fall, the tropopause backs away from the high radioactivity concentrations. Staley (1962) showed that the combination of seasonal mass exchange and seasonal change of radioactivity concentration at the tropopause associated with its seasonal height variations has the qualitative effect of delaying the time of maximum transport into the troposphere. The amount of delay depends on the relative importance of the two effects.

The possible effect of seasonal variation of stratospheric mass was further investigated by Staley (1963a) by overlaying a time-latitude section of 1957–58 (IGY years) stratospheric mass incorporation into the troposphere on a time-latitude section of 1960–61 fission-product gross beta activity in surface air. At middle and high latitudes of the Northern Hemisphere, the patterns are similar and tend to coincide. The spring maximum of high activity is delayed with increasing latitude, as is also the simultaneous maximum of mass incorporation, corresponding to a tropopause that rises first at lower middle latitudes in late winter or early spring, and rises later at higher latitudes. The jet stream was also shown to move northward during spring, with its position falling on top of the maxima of mass incorporation and radioactivity concentration at the

surface. In the Southern Hemisphere, there was some correlation of the maxima in lower middle latitudes, but the concentration of radioactivity in surface air of the Southern Hemisphere was small and seasonal patterns ill-defined at this time, since the principal sources of radioactivity were in the Northern Hemisphere. In the tropics, a small (<20 mb in 2 months) variation of tropopause height occurred at the same time in both hemispheres, specifically a falling tropopause from February to August and a mostly rising tropopause from August through January.

The other effect which has been cited as important for producing a spring maximum of radioactivity in surface air and deposition on the surface is transport within the stratosphere. It has long been accepted that the spring increase of total ozone is related to seasonal variation of mass transport in the stratosphere, with photochemical production replacing ozone, which is transported downward, resulting in higher total O_3. A time-latitude section of zonal-mean O_3 by Dütsch (1969) shows spring maxima in the Northern and Southern Hemispheres. Total fission-product radioactivity, of course, is not affected by stratospheric transport. However, such transport can affect concentrations at the tropopause and, in turn, transport into the troposphere where radioactivity is rapidly scavenged. Concentrations in the troposphere can subsequently show large seasonal variations.

2. Purpose

Kida (1977a,b) and Mahlman and Moxim (1978) have numerically simulated atmospheric tracer transport. It is to be expected that improved simulations of tracer transport will be forthcoming. In order to have detailed and reliable radioactivity distributions with which to compare simulations, it is desirable to make maximum use of available measurements. Monthly mean Sr-90 concentrations in surface air were measured along the 80th meridian from 1963 to 1975 (after which low concentrations caused a change to reporting of quarterly values), and have been tabulated by Feely *et al.* (1980). However, they have been subjected to little statistical analysis. During this period, the stratospheric inventory decreased by more than an order of magnitude, due to transport to the troposphere, and fluctuated considerably due to recurrent atmospheric testing of high-yield nuclear weapons.

The purpose of this paper is to analyze this long Sr-90 time series, in order to distill a characteristic global and seasonal variation suitable for testing tracer transport models, and to identify, from the patterns, the major physical processes that must be included in a successful model. The seasonal variation of Sr-90 in surface air turns out to be remarkably constant year after year, and little affected by the magnitude of the stratospheric inventory. Seasonal patterns of Sr-90 concentration in the tropics turn out to be influenced by seasonal variations of precipitation rate.

3. Stratospheric inventory of Sr-90

The immediate source of Sr-90 in surface air is Sr-90 in the stratosphere. To understand the general trend of concentrations in surface air over the period 1963–75, it is useful to consider first the stratospheric inventory of Sr-90 during this period. Fig. 1 shows northern, southern, northern minus southern, and total stratospheric inventories, as well as the large atmospheric tests that contributed to these inventories, adapted from figures shown by Leifer *et al.* (1976, 1979).

From January 1963 to middle 1967, no large-yield testing occurred. At the start of this period, the inventory in the Northern Hemisphere stratosphere exceeded that in the Southern Hemisphere by almost an order of magnitude. Initially, throughout most of 1963, the Southern Hemisphere stratospheric burden increased as transport to it from the Northern Hemisphere stratosphere exceeded its loss to the troposphere. Transfer from the Northern Hemisphere stratosphere continued through 1966, at which time the inventory of Sr-90 in the Southern Hemisphere stratosphere equalled that in the Northern Hemisphere.

From 1967 through 1972, the Northern and Southern stratospheric inventories take turns exceeding each other, according to the hemisphere of recent testing. After testing in mid-1973, the variations in both hemispheres resemble their behaviors in 1963 after the testing of December 1962. In both cases, the Southern Hemisphere inventory increases for a few months as interhemispheric transfer occurs, then decreases as transfer into the troposphere begins to dominate.

Although radioactivity is not well-mixed vertically in the stratosphere, the more or less straight curves during nontesting periods for B_N, B_S and $B_N - B_S$, where B_N and B_S are the burdens in the Northern and Southern Hemisphere, respectively, suggest that to a first approximation the transfer processes are linear, and that transfer can be described by

$$\frac{dB_N}{dt} = -\lambda_T(B_N - B_1) - \lambda_E(B_N - B_S) - \lambda_{Sr}B_N \approx -(\lambda_T + \lambda_{Sr})B_N - \lambda_E(B_N - B_S), \quad (1)$$

$$\frac{dB_S}{dt} = -\lambda_T(B_S - B_2) + \lambda_E(B_N - B_S) - \lambda_{Sr}B_N \approx -(\lambda_T + \lambda_{Sr})B_S + \lambda_E(B_N - B_S), \quad (2)$$

where λ_T, λ_E, λ_{Sr} are decay constants for transfer across the tropopause, transfer across the equator,

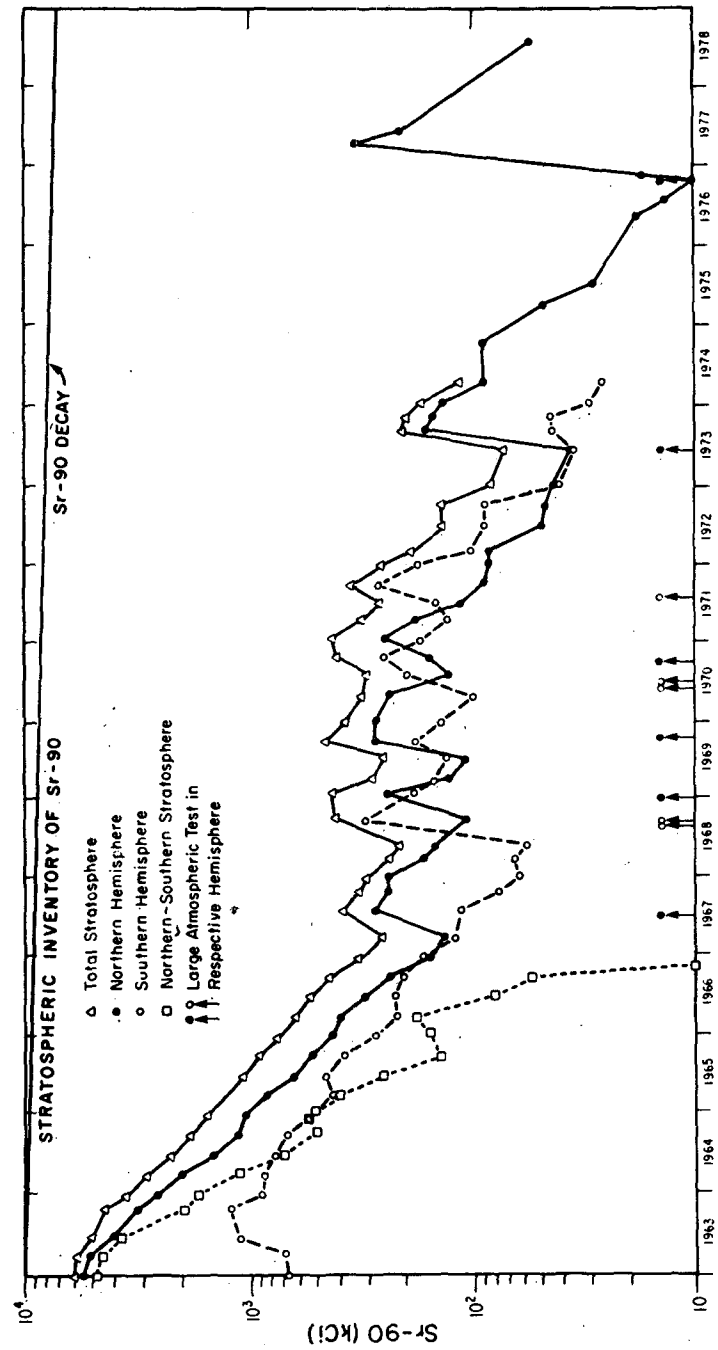

FIG. 1. Stratospheric inventory of Sr-90 from 1963 to 1978 (after Leifer *et al.*, 1976, 1979).

and decay of Sr-90, respectively; and B_1 ($\ll B_N$) and B_2 ($\ll B_S$) are tropospheric burdens in the Northern and Southern Hemisphere, respectively. (B_1 and B_2, rather than being actual burdens, should be scaled down to adjust for the larger tropospheric mass.) The radioactive decay of Sr-90 is small compared to the effect of transfer, but can be retained without causing difficulty.

Subtraction of (2) from (1) yields

$$\frac{dD}{dt} = -\lambda_* D, \tag{3}$$

where $D \equiv B_N - B_S$ and $\lambda_* \equiv \lambda_T + \lambda_{Sr} + 2\lambda_E$. The decay constants are related to residence half-times or radioactive half-life according to

$$T_{1/2*} \equiv \frac{0.693}{\lambda_*}, \quad T_{1/2T} \equiv \frac{0.693}{\lambda_T},$$

$$T_{1/2E} \equiv \frac{0.693}{\lambda_E}, \quad T_{1/2Sr} \equiv \frac{0.693}{\lambda_{Sr}}.$$

The solution of (3) is

$$T_{1/2*} = \frac{0.693(t - t_0)}{\ln(D_0/D)}, \tag{4}$$

where D_0 corresponds to t_0. For t_0 corresponding to 1 January 1963 and t = 1, 2, 3 years, $T_{1/2*}$ turns out to be 0.63, 0.61 and 0.61 years, respectively. For t_0 corresponding to 1 January 1964 and t = 1, 2 years, $T_{1/2*}$ turns out to be 0.57 and 0.50 years, respectively. Thus the half-life for decay of $B_N - B_S$, according to Fig. 1, was of the order of 7–8 months in 1963, but decreased in 1964 and 1965 to 6–7 months. This time is shorter than stratospheric half-residence times (see below); it reflects not only mass transfer between hemispheres, which decreases B_N while increasing B_S, but also transfer to the troposphere and decay, which act selectively on the stratosphere with the larger burden.

If (1) and (2) are added, we find

$$\frac{dB_T}{dt} = -(\lambda_T + \lambda_{Sr})B_T, \tag{5}$$

where $B_T \equiv B_N + B_S$ is the total stratospheric burden. The solution for the residence half-time for transfer from stratosphere to troposphere is

$$T_{1/2T} = \frac{0.693 T_{1/2Sr}(t - t_0)}{T_{1/2Sr} \ln(B_{T_0}/B_T) - 0.693}. \tag{6}$$

For t_0 corresponding to 1 January 1963 and t to 1 January 1964, Eq. (6) yields $T_{1/2T}$ = 1.34 years. During the first part of 1963, the flatness of the inventory curves in Fig. 1 suggests that radioactivity from the 1962 tests had not yet spread enough for removal to be effective and in constant proportion to the inventory. For t_0 corresponding to 1 January 1964 and t = 1, 2, 3 years, we find $T_{1/2T}$ = 0.86, 0.88 and 0.87 years, respectively. Thus the half-residence time for transfer from stratosphere to troposphere, according to Fig. 1, was ~16 months in 1963, but ~10.5 months in 1964, 1965 and 1966. The latter value compares with 10 months found by Feely *et al.* (1966) from Sr-90 data for 1963, 1964.

From the definition of λ_*, the residence half-time for interhemispheric transfer within the stratosphere may be expressed as

$$T_{1/2E} = \frac{2T_{1/2*}T_{1/2T}T_{1/2Sr}}{T_{1/2Sr}T_{1/2T} - T_{1/2*}T_{1/2Sr} - T_{1/2*}T_{1/2T}}. \tag{7}$$

For $T_{1/2Sr}$ = 28.82 years, $T_{1/2T}$ = 0.87 years and $T_{1/2*}$ = 0.50 years, it follows that $T_{1/2E}$ = 2.4 years, while for $T_{1/2*}$ = 0.57 years, we find $T_{1/2E}$ = 3.5 years. This compares with 1.4–2.3 years found by Junge (1963) for interhemispheric mixing of CO_2 and tritiated methane (CH_3T) within the troposphere, with stratospheric exchange included.

If the Northern Hemisphere curve in Fig. 1 is assumed to be straight, implying

$$\frac{dB_N}{dt} = -\frac{0.693}{T_{1/2N}} B_N, \tag{8}$$

the burdens from January 1964 to January 1966 or January 1967 imply $T_{1/2N}$ = 9.5 and 9.1 months, respectively. This is about a month less than $T_{1/2T}$, smaller because it includes the slow loss to the Southern Hemisphere.[1] Fabian *et al.* (1968) expressed Sr-90 concentration in rain at 48 stations of the Northern Hemisphere for the period 1964–66, after removal of seasonal trends, as an exponentially decreasing function of time. The average value of the half-life of this decay turned out to be 9.4 months. This half-life reflects not only transfer from stratosphere to troposphere, but also interhemispheric exchange in the stratosphere and troposphere. This half-life, therefore, is physically the same as $T_{1/2N}$ with the exception of tropospheric interhemispheric exchange, which is probably small (because of rain scavenging, especially in the equatorial rain belt), compared to stratospheric exchange.

The implications of Fig. 1 can be summarized by the internal inequalities and magnitudes in

[1] Eq. (1) implies that dB_N/dt is not actually expressible as dB_N/dt = −constant × B_N except when $B_S \ll B_N$. During much of 1963 to 1967, B_S was less than B_N, and if B_S is neglected, the constant in this expression is $\lambda_T + \lambda_{Sr} + \lambda_E$. If this is equated to $0.693/T_{1/2N}$, we find $T_{1/2N}$ = 7.5 and 10.8 months for $T_{1/2T}$ = 0.87 years and $T_{1/2E}$ = 2.4 and 3.5 years, respectively.

$$T_{½R} < T_{½*} < T_{½N} < T_{½T} < T_{½E} < T_{½Sr} \quad (9)$$

≤0.7 month	6–7 months	9–10 months	10–11 months	2.5–3.5 years	28.8 years
(tropospheric scavenging of radioactivity)	(decay of NH-SH inventory difference)	(decay of NH inventory by transfer to troposphere and SH)	(decay of NH + SH inventory)	(decay of NH inventory by transfer to SH alone)	(radioactive decay of Sr-90)

The first and last quantities are added for perspective.

Fabian *et al.* (1968) solved the system (1), (2), but related stratospheric inventories to Sr-90 concentration in rain by means of a "transfer coefficient," in order to find values for the inventories. This indirect procedure, subject to various assumptions and applied to selected stations, yielded the means $\bar{T}_{1/2T} = 13$ months and $\bar{T}_{1/2E} = 2.3$ years, values slightly larger and smaller, respectively, than those found here.

On the basis of three Chinese tests between June 1967 and September 1969, Machta and Telegadas (1973) found $T_{1/2T}$ to be 16 months for the fall-winter period, 7 months for winter-to-spring, 9 months for spring-to-summer, and 11 months for summer-to-fall. The average is 10.8 months, in agreement with the more or less average value found from Fig. 1, which does not have nearly enough detail to allow computations of seasonal value.

The smoothness in Fig. 1 of the Northern Hemisphere and total atmosphere curves in the early years reflects an integration of measurements that is insensitive to seasonal variations. These should be large because the seasonal variations of Sr-90 concentration in surface air are large and must reflect (except in the tropics, as discussed in Section 8) a large seasonal variation in transport across the tropopause. Krey and Krajewsky (1972) report that the stratospheric burden was equated to nuclide content above 180 mb. For the determination of average residence times, this poses no difficulty, but the indicated inventories are not true stratospheric inventories.

4. Seasonal variations of Sr-90 in surface air

Feely *et al.* (1980) have tabulated monthly mean values of concentrations in surface air along the 80th meridian for the years 1963–75. Concentrations are also given at a few locations at other longitudes for a shorter span of years within this period. After 1975, concentrations at many locations became so low that only quarterly means were given. Hence, in order to make a detailed study of seasonal variations, measurements after 1975 are excluded here.

At each measuring station, an annual mean of the 12 monthly means was first computed for each year. Next, the percentage departure from the annual mean was computed for each month of every year. Next, mean monthly percentage departures were computed for the years 1963–75. The results can now be plotted as a latitude-time section of average monthly percentage departure from the annual concentration means.

However, the pattern would be distorted by the long-term decrease in Sr-90 concentrations, especially those that occurred during 1963–66. At Sterling, Virginia, for example, the mean annual surface concentration decreased from 65.0 to 5.25 fCi m^{-3}. If there were no seasonal variations at all, the pattern would show positive percentage deviations in the first half of the year and negative deviations in the second half. Therefore, the mean percentage departures for each month were corrected for the decrease of the annual means. (The large decrease of surface air concentration over the years, especially from 1963 to 1966, is the reason average concentrations for each month of the year were not computed. Disproportionate weight would have been given to seasonal variations in early years of high concentration.) The results for 1963–75 are shown in Fig. 2. The pattern is actually very similar to that (not shown here) which is obtained without separating out the distortion of the long-term decrease of concentration, which shows that seasonal meteorological effects dominate.

Before discussing Fig. 2, it should be pointed out that occasional monthly mean concentrations in the Feely *et al.* data were missing, or else described as having an error in the range from 20 to 100%. If only one or two consecutive monthly values were missing, values were interpolated between previous and following months. If several months were missing, the whole year could not be used. If the error was indicated, the value was used if it appeared to be consistent with the preceding and following months. This was almost always the case. If the value appeared out of line by being much larger than preceding and following values, it was assumed that it was indeed in error by a large percent. It was then discarded and replaced by an interpolated concentration. This occurred in only two instances along the 80th meridian. If the tabulated monthly concentration was very small compared to the tentative annual mean and indicated as being in error, the value was used anyway, since even if it were in error by 100%, the corrected value would still be small (and not

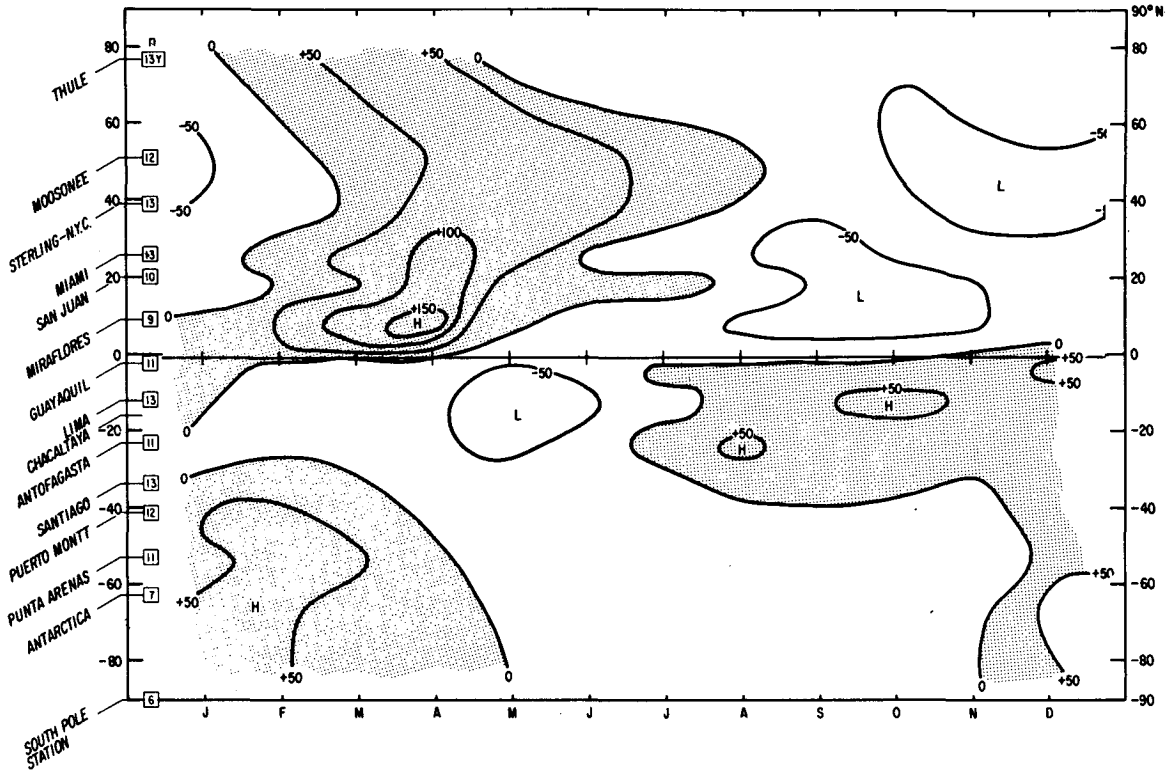

FIG. 2. Mean percentage departures of Sr-90 concentration in surface air from annual means for the period 1963–75, corrected for interannual trend. Stations near the 80th meridian are shown on left; *n* is period of record in years.

given by interpolation), and the percentage departure from the annual mean would be little affected. Altogether only some 50 concentrations out of a total of more than 1500 were interpolated. Errors were not given for individual measurements, except, as noted above, when they exceeded 20%. In what follows, it will be assumed that individual values given by Feely *et al.*, as well as interpolated values, are true monthly means.

Fig. 2 shows the expected spring maximum and fall minimum in the Northern Hemisphere. However, the extremes of percentage departure occur at the lowest latitude station, Miraflores (9°N).

In the Southern Hemisphere, the spring maximum is more of an extended late winter maximum. It is also more confined to lower latitudes, although a separate maximum occurs in summer at a higher latitude. The extremes of percentage departure in the Southern Hemisphere also occur close to the equator.

Although Chacaltaya (16°21′S) is part of the 80th meridian network, it was not used in the analysis. This station is at 5220 m, much higher than the remaining stations. Concentrations tended to be much larger and more erratic than those for nearby stations, especially Lima. Therefore, it was removed as being unrepresentative.

Fig. 2 shows that characteristic hemispheric seasonality extends as close to the equator within each hemisphere as there are stations to detect it. The largest percentage departures occur near the equator at Miraflores (9°00′N) and Lima (12°01′S). The phase at Guayaquil (2°10′S) is approximately 6 months different from that at Miraflores, and departures at Guayaquil show qualitatively the same seasonality that extends to middle latitudes of the Southern Hemisphere.

However, within the limits of the data, the seasonality is also symmetric with respect to the position of the equatorial trough (i.e., the ITCZ) which separates the meteorological hemispheres. Riehl (1979) shows the July and January positions of the trough (at 80°W) at ~7°N and ~3°N, respectively. Thus, the meteorological equator appears to be located roughly midway between Miraflores and Guayaquil throughout the year.

Perhaps the most remarkable aspect of the spring maximum is that it appears at Miraflores *before* it appears at stations farther north. This delay of the spring maximum is brought into sharper focus in Fig. 3, which shows seasonal variations of percentage deviation at Miraflores (9°N), Miami (26°N) and Sterling–New York City (39, 41°N). Thus, the spring maximum at the lowest latitudes of the Northern Hemisphere cannot be regarded as having propagated southward through the troposphere from regions where a spring maximum appeared earlier. On

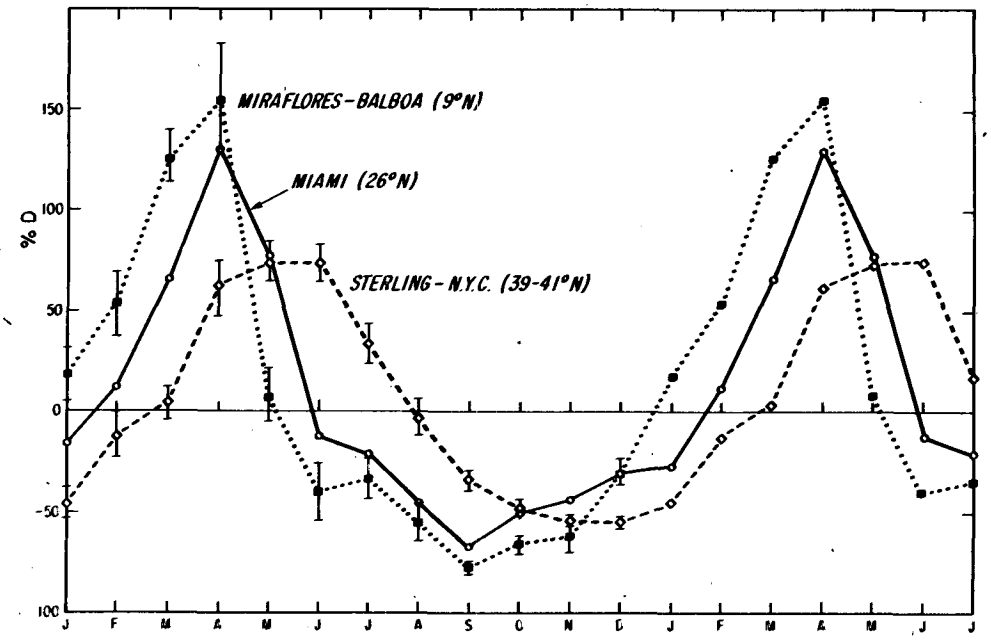

FIG. 3. Mean percentage departures of Sr-90 concentration in surface air from annual means at selected stations of the 80th meridian network for the period 1963–75. Standard error $\sigma n^{-1/2}$ for Miami is shown in Fig. 6.

the other hand, propagation northward of a pulse of activity introduced near the equator cannot be inferred either, since, if magnitudes of activity are introduced, the amplitude decreases toward the equator. Prevailing winds should be toward the ITCZ in the latitudes just north of Miraflores, advecting radioactivity southward toward Miraflores. Thus the early maximum at Miraflores is indeed difficult to account for on the basis of horizontal advection.

The plots in Fig. 3 are repeated for another 7 months to show that the spring maximum is more sharply peaked upward than the fall minimum downward.

Referring again to Fig. 2, we see that the time of the Northern Hemisphere maximum is delayed with increasing latitude up to ~50°N, beyond which the maximum is reached earlier. The behavior below 50°N was noted by Staley (1962, 1963a,b) in much less data, and must be regarded as a very characteristic feature, at least near 80°W. As noted in Section 1, this feature coincides with the seasonal decrease of stratospheric mass and northward shift of the jet stream.

The spring maximum in the Southern Hemisphere is much more diffuse and confined to latitudes less than 40°. It does not show any delay as latitude is increased.

A summer maximum occurs at high latitudes of the Southern Hemisphere. There seems to be no counterpart of this in the Northern Hemisphere.

The minima in both hemispheres are flattish. In the Southern Hemisphere, the minimum occurs in late fall at low latitudes and is delayed into winter, and even late winter, with increasing latitude.

Fig. 4 shows the result of computing average percentage departures for only the years 1963–66 and retaining Chacaltaya. Corrections were again made for the decrease of annual means, which was large over this period. The pattern is similar to that in Fig. 2 for the much longer period, although the Southern Hemisphere maxima and minima are concentrated at the latitude of Chacaltaya for reasons mentioned before. The similarity of the average departures for the first four years to the average departures for the complete 13-year period indicates that seasonal trends are largely independent of the stratospheric burden. There may also have been a change in the height or latitude of the center of mass of the radioactivity, but, if so, it made little change in the seasonal variation of radioactivity in surface air.

Figs. 2–4, showing mean percentage departures of concentration, do not reveal the variation of concentration magnitude with latitude. Although the magnitude of concentration varies greatly, depending on weapon yield and on the time elapsed since testing, the profile of mean annual concentration within a hemisphere varies little from year to year. To construct a time-latitude section showing concentration, the annual mean concentration of one station in each hemisphere (New York City–Sterling in the Northern Hemisphere, Santiago in the Southern) was arbitrarily assigned, every year, the value unity. Each year the annual means of other stations in that hemisphere were expressed as fractions of unity. Average

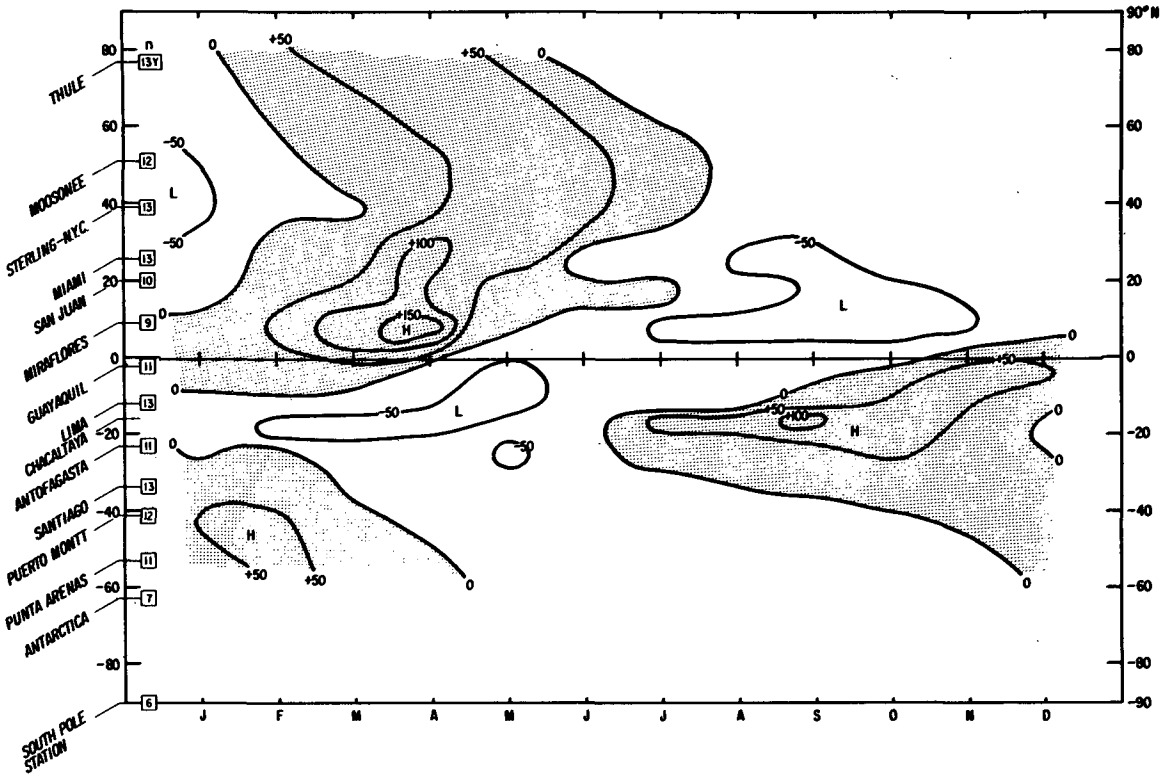

FIG. 4. As in Fig. 2 but for the period 1963–66.

annual means over three years were then obtained for all stations in the hemisphere and are presented in Table 1. Note that the standard errors are small. The percentage departures in Fig. 2 were next scaled by the appropriate average annual mean from Table 1 to construct a concentration for each month. By this procedure, any interannual variation of concentration, and most of the interhemispheric differences of concentration, are removed, leaving a time-latitude section of concentration based on many years of data. If the stratospheric burden of radioactivity were maintained at the same level throughout the

TABLE 1. Average profile of annual mean Sr-90 concentrations in surface air. Means at New York City-Sterling and Santiago are arbitrarily given the value unity every year, and means at other stations within each hemisphere are expressed as fractions of unity. $n = 5$ at South Pole, $n = 8$ at Antarctica, otherwise $11 \leq n \leq 13$.

Stations	Latitude	Average annual mean	Standard deviation σ of annual means	Standard error $\sigma n^{-1/2}$
Thule, Greenland	76°36′N	0.789	0.123	0.034
Moosonee, Ontario	51°16′N	0.837	0.154	0.043
New York City, New York Sterling, Virginia	40°44′N 38°58′N	1.000	—	—
Miami, Florida	25°49′N	1.004	0.189	0.052
San Juan, Puerto Rico	18°26′N	0.750	0.127	0.038
Miraflores, Canal Zone Balboa, Canal Zone	9°00′N 8°58′N	0.349	0.091	0.027
Guayaquil, Ecuador	2°10′S	0.289	0.152	0.044
Lima, Peru	12°01′S	1.064	0.217	0.060
Antofagasta, Chile	23°37′S	1.090	0.201	0.058
Santiago, Chile	33°28′S	1.000	—	—
Puerto Montt, Chile	41°27′S	0.558	0.061	0.017
Punta Arenas, Chile	53°08′S	0.329	0.055	0.017
Antarctica	62°56′S 64°49′S	0.331	0.119	0.042
South Pole Station	90°00′S	0.658	0.141	0.063

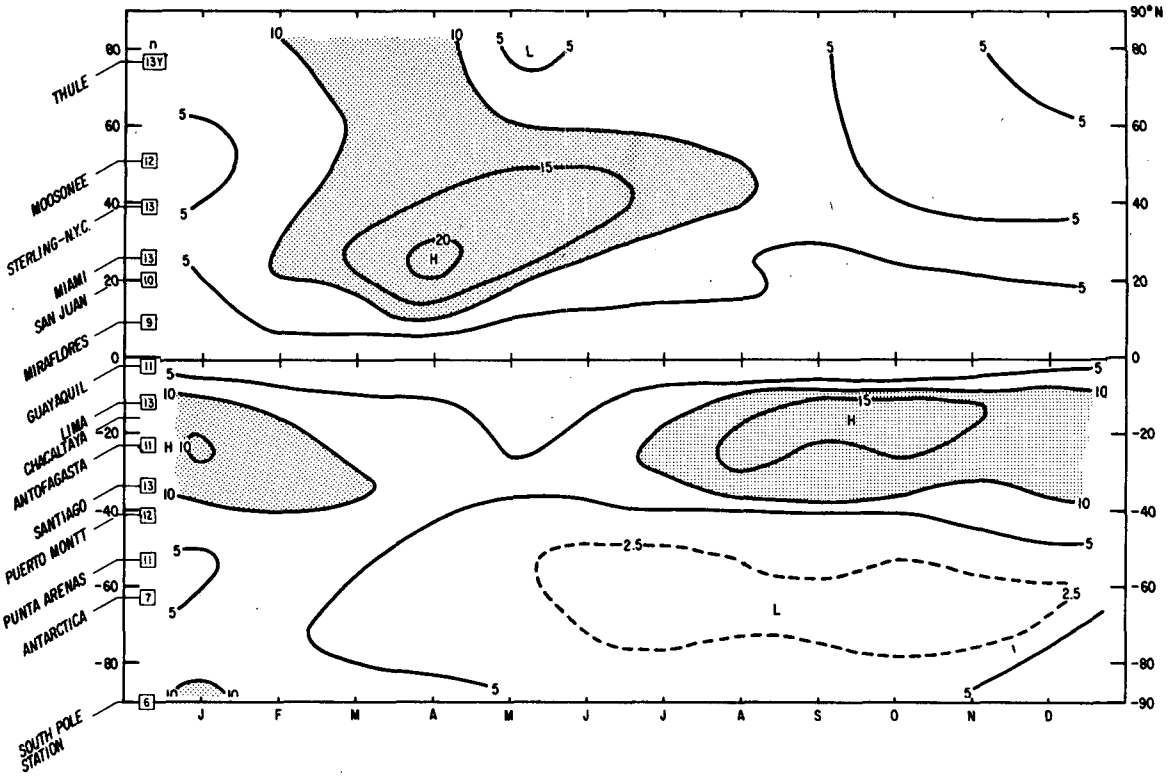

FIG. 5. Observed concentration of Sr-90 in surface air based on mean monthly percentage departures from mean (1963–75) latitudinal profiles of concentration and with interannual trend removed. Magnitudes separately arbitrary in each hemisphere.

year, surface concentrations should resemble this time-latitude section. The results are shown in Fig. 5, in which the concentration units are separately arbitrary in each hemisphere. (There is no significance to any numerical differences between maxima or minima compared across the equator.)

Comparison of Fig. 5 with Fig. 2 shows that the spring maxima of concentration occur farther from the equator than the spring maxima of percentage departure (~25°N as compared to ~10°N, and ~15–25°S as compared to ~10–15°S). The latitudes of maximum concentration of radioactivity, in turn, are much less than those of the spring maxima of total ozone, which are found at 90°N and 50°S (Dütsch, 1969). They are also found at lower latitudes than the middle- and high-latitude maxima of tropospheric ozone shown by Fabian and Pruchniewicz (1977).

As in Figs. 2 and 3, the spring maximum in the Northern Hemisphere is delayed with increasing latitude in lower-middle latitudes. The maximum at high latitude occurs at about the same time as at lower-middle latitudes.

A minimum of concentration occurs throughout the year at the equator. This minimum tends to obscure the seasonality revealed by Figs. 2 and 3.

In the Southern Hemisphere, a flattish spring maximum occurs in the subtropics, but an even flatter late winter and spring minimum occurs in upper middle latitudes. The late summer maximum at high latitudes that appeared in the percentage departures of Fig. 2 is much reduced but still in evidence in Fig. 5.

No closed low centers of concentration occur between the equator and midlatitudes of either hemisphere, in contrast to the patterns of percent departure.

5. Distribution of standard error

Fig. 6 shows the distribution of standard error $[\sigma n^{-1/2}]$ where σ is the standard deviation of the mean percentage departures shown in Fig. 2, and n the number of years used, as shown on the left. Comparison with Fig. 2 shows that the smallest errors are associated with negative percentage deviations. Some of these errors are remarkably small—the smallest being only 2%.

Larger errors are associated with regions of positive percentage departures, but even these are small compared to the amplitude of percentage departures themselves.

The pattern of error is similar to the pattern of percentage departure, but more erratic. This is

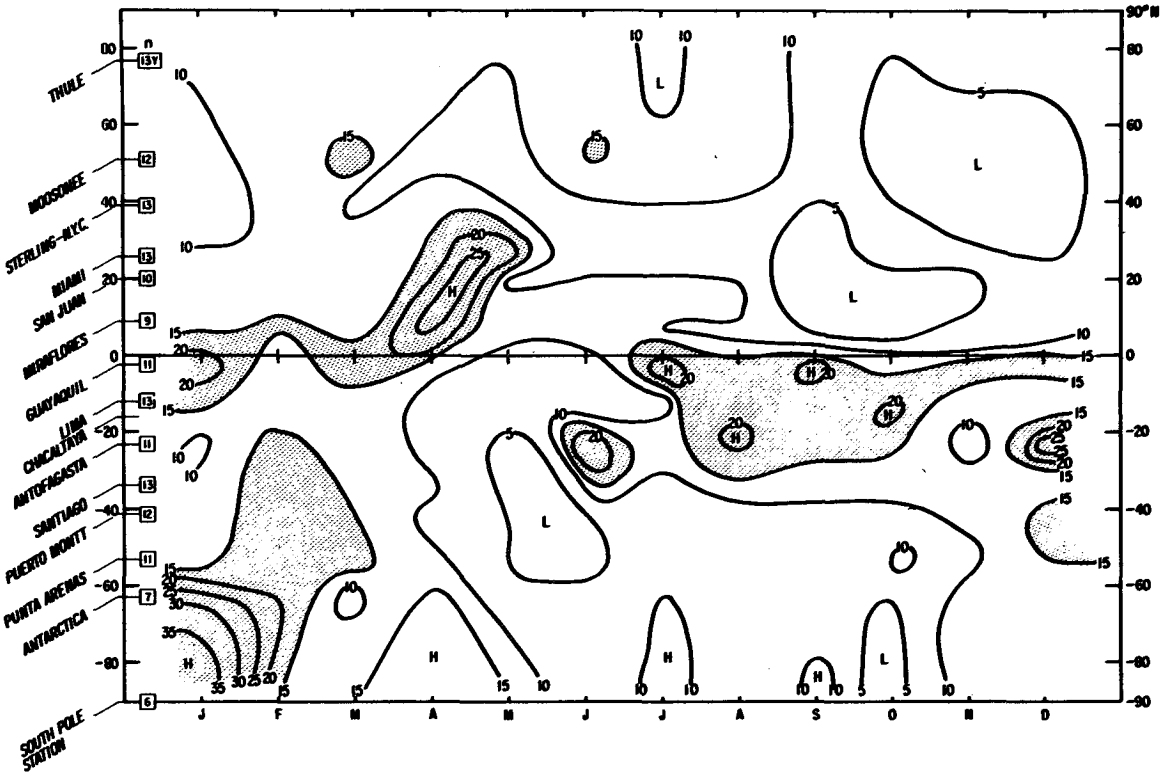

FIG. 6. Distribution of standard error $\sigma n^{-1/2}$ for the mean percentage departures shown in Fig. 2. Number of years n is shown on left.

mostly related to an occasional percentage departure that is considerably different from the remaining departures. There seems to be no obvious explanation for these occasionally anomalous departures. One of these cases occurs at Antofagasta in June 1967, when the percentage departure from the annual mean was +226%. All other June percentage departures for the remaining 10 years were negative. Typographical errors in the tabulated data, especially involving decimal points, seem a possibility, but are not strongly suggested. In the case of Antofagasta, 7 of 11 percentage departures in July are positive, indicating a winter transition from negative to positive departures from mean annual concentrations. The question of whether or not June 1967 was climatologically anomalous at Antofagasta naturally arises, but the answer goes beyond the scope of this paper. Telegadas (1981, personal communication) has pointed out an anomaly in the Ce-144 to Sr-90 activity ratio for June 1967 at Antofagasta and suggests the reported Sr-90 concentration was incorrect and probably an order of magnitude too large. The original radiochemical analysis seems to be unavailable.

The general similarity of the standard error distribution in Fig. 6 to the Sr-90 distribution in Fig. 2 is probably largely a consequence of precipitation scavenging rates being more variable from one spring to the next than from one fall to the next. As argued in Section 8, the scavenging half-life is inversely proportional to precipitation rate P. The standard deviation of P^{-1} computed for low-precipitation months (using several years of data) is many times larger than the standard deviation of P^{-1} for months with high precipitation. Hence, to the extent that Sr-90 concentration represents an equilibrium between local precipitation scavenging and sources (related to transport), Sr-90 concentration will show much more interannual variability between relatively dry months than relatively wet months. (See Figs. 13 and 16 for precipitation data.) Variability of dry deposition may also contribute to the standard error, but this contribution should be small compared to that of wet removal.

Tropospheric debris from specific tests also contribute to the standard error. At lower latitudes, such tests apparently make a smaller contribution to the standard error than the variability of precipitation scavenging.

6. Interhemispheric comparisons of Sr-90 seasonality

Fig. 7 compares the percentage deviations across the equator, using the stations nearest the equator

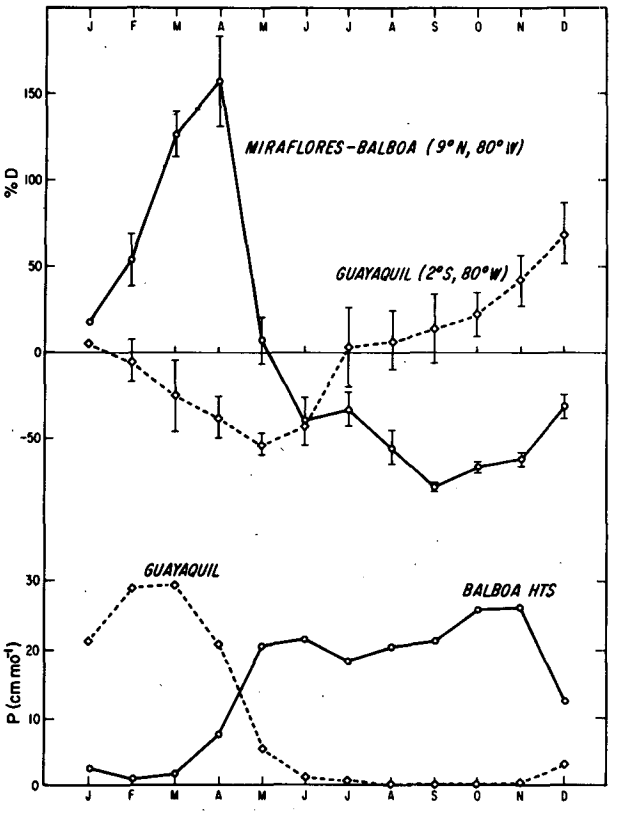

FIG. 7. Mean percentage departures of Sr-90 concentration in surface air from annual means for the period 1963–75 at the two stations closest to the equator in each hemisphere. Corrected for interannual trend, as in Fig. 2. Standard error bars from Fig. 6. Lower curves are precipitation rate at these stations.

in each hemisphere. Even though Guayaquil is only 2° from the equator, it shows clearly the characteristic seasonal variation of other stations between the equator and 40°S.

Also shown in Fig. 7 are precipitation rates. Note the large amplitude of precipitation-rate fluctuations and the generally negative correlation with radioactivity. More on this in Section 8.

Fig. 8 compares San Juan (18°N) with Lima (12°S). The spring maximum and fall minimum are well-defined at both stations. The association of relatively large standard error with positive deviations and relatively small error with negative deviations is also evident.

Fig. 9 compares Moosonee (50°N) with Punta Arenas (53°S). At Punta Arenas, the spring maximum and fall minimum of lower latitudes have been replaced by a late summer maximum and a winter minimum, consistent with the abrupt latitudinal phase change noted in Fig. 2.

7. Longitudinial comparisons of Sr-90 seasonality

The radioactivity sampling network was criticized early for being restricted to a narrow range of longitude near the 80th meridian (W) and for being either along an east coast (Northern Hemisphere) or along a west coast (Southern Hemisphere). The extent to which radioactivity concentrations were truly representative of their latitude was therefore in doubt. The addition of a few more stations at other longitudes shows that longitude plays a secondary

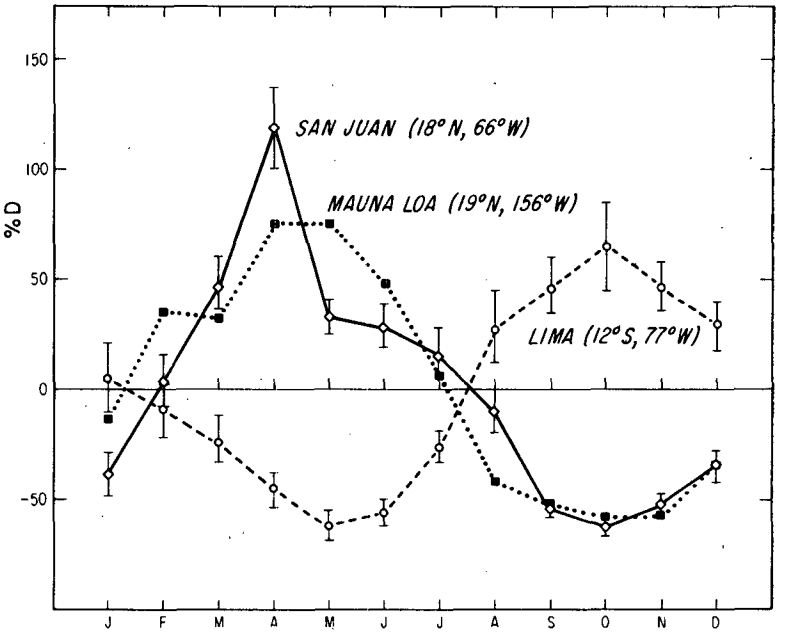

FIG. 8. As in Fig. 7 but for two stations, San Juan and Lima, about 15° north and south of the equator, respectively. Mauna Loa is shown for longitudinal comparison with San Juan. Mauna Loa error bars are similar to those at San Juan.

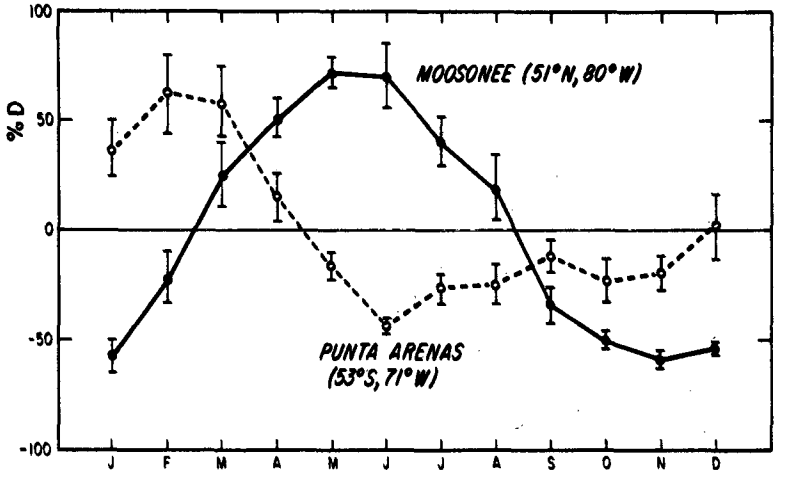

FIG. 9. As in Fig. 7 but for two stations, Moosonee and Punta Arenas, about 52° north and south of the equator.

role at some latitudes, but not enough stations were added to resolve the question at others.

Mauna Loa (19°28′N, 155°36′W) is compared in Fig. 8 with San Juan (18°26′N, 66°00′W). Although Mauna Loa is at 3401 m as compared to 10 m for San Juan, the curves are very similar.

Easter Island (27°10′S, 109°26′W; 5 years of data, 1971–75, inclusive) is compared in Fig. 10 with Santiago (33°28′S, 70°42′W). The curves are again very similar.

Salt Lake City (40°46′N, 110°49′W) is compared in Fig. 11 with Sterling-New York City (~40°N, 76°W). Again, the curves are very similar, the only significant difference being the larger spring maximum at Salt Lake City. This may be related to the substantially greater elevation of Salt Lake City.

Unfortunately, there were no additional measurements at other longitudes near the equator with which to compare those at Miraflores-Balboa and Guayaquil. As shown in Section 8, the seasonality at these stations is closely related to rainfall rate, which, in turn, relates well to seasonal excursions of the equatorial trough that extends around the earth. Hence the pronounced seasonality found near the equator along the 80th meridian is probably representative of other longitudes.

There are very few data at other longitudes suitable for comparison with Lima, Chacaltaya and Antofagasta on the very dry west coast of South America. This is unfortunate because of the effect of precipitation scavenging on surface air concentrations, as shown in the next section.

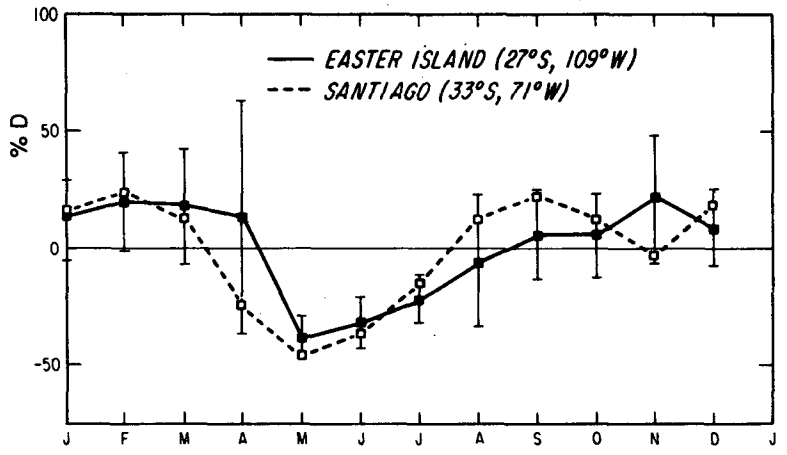

FIG. 10. Mean percentage departures of Sr-90 concentration in surface air from annual means for the period 1963–75 at two stations near 30°S, but at very different longitudes. Five years' data at Easter Island, thirteen at Santiago. See Fig. 6 for Santiago errors.

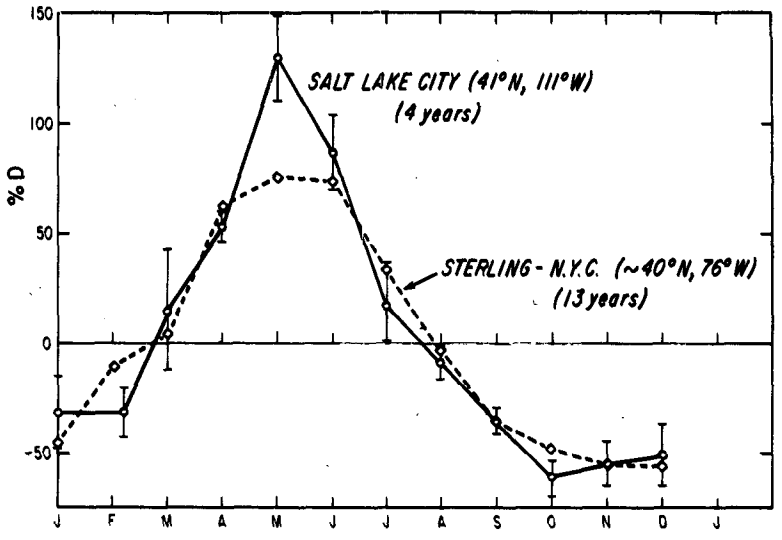

FIG. 11. As in Fig. 10 but for stations near 40°N. See Fig. 6 for Sterling-New York City errors.

8. Effect of precipitation seasonality

Because of spatial variation of radioactivity concentration, the sort of formulation used in (1) and (2) is not suitable for describing the variation of concentration at particular locations. The removal of particulate matter is primarily by precipitation scavenging, and this fact suggests that seasonal variation of precipitation should contribute to seasonal variation of Sr-90 concentration in surface air. This effect should be in addition to those of seasonal transport within the stratosphere and seasonal changes of stratospheric mass. Let C be the concentration of Sr-90 in surface air. In areas where precipitation rate undergoes a large seasonal variation, the concentration in surface air should be described by

$$\frac{\partial C}{\partial t} = -kP(t)C + S(t), \qquad (10)$$

where k is a constant, $P(t)$ the precipitation rate, $kP(t)$ a decay factor, and $S(t)$ a source, related to transport within the troposphere and, more remotely, to transport within the stratosphere and seasonal changes of stratospheric mass. To focus attention on the effect of seasonal variation of precipitation rate, in what follows, we set $S(t)$ = constant.

Junge (1963) shows that the mean residence time of aerosols, if distributed uniformly with height, is inversely proportional to the daily rainfall rate. Specifically, for a cloud liquid-water content of 2 g m^{-3}, the residence times for daily rainfall rates of 0.12, 0.25 and 0.50 cm were 16.6, 8.0 and 4.0 days, respectively. At Balboa, in February, the precipitation rate is only 0.4 cm month^{-1}. Extrapolation of the Junge relationship yields a mean aerosol residence time of 5 months. In October and November, the precipitation rate at Balboa is about 25 cm month^{-1}, corresponding to a mean aerosol residence time of less than 3 days. For three or more months at Guayaquil and Lima, the precipitation rate is less than 0.13 cm month^{-1}, yielding an aerosol mean residence time for wet removal of more than 15 months. Hence, during periods of low precipitation rate, such as occur at some stations along the 80th meridian, the aerosol mean residence time would be of the order of months if wet removal were the only effect. During periods of moderate or high rainfall, the aerosol mean residence time may be only a few days. Junge reasons that the mean residence time for fission products, whose concentration increases with height, will be somewhat longer.

Martell and Moore (1974) find somewhat smaller aerosol residence times than those found or endorsed by Junge. From the Bi-210/Pb-210 activity ratio and Pb-210 versus altitude, they find half-residence times of less than a week over the western United States. It is clear that aerosol residence half-life is extremely variable, depending on precipitation rate.

For Sr-90, the mean residence time is $[kP(t)]^{-1}$ in (10), and the half-residence time is 0.693 $[kP(t)]^{-1}$. The inverse proportionality to precipitation rate is the same as that found by Junge. Where precipitation rate varies widely, the half-residence time may vary from a day or two to months.

As a numerical example, let $P(t) = 10 + 9.6 \cos\nu t$ [cm month^{-1}], where $\nu = (2\pi/12)$ months, $k = 0.1$ cm^{-1} and $S = 30$ arbitrary units per month. For these values, the half-life for concentration decay ranges from 0.35 month when $P(t)$ is at a minimum to 17.3 month when $P(t)$ is at a maximum. The value of S is arbitrary. Analytical solution of (10) is difficult,

so it was solved numerically using forward integration with 0.5 months time increments.

The results, expressed as concentration versus precipitation rate, are shown in Fig. 12. Three different initial conditions were used: $C_0 = 5$ and 50 for $P(0) = 19.6$ cm month^{-1} and $C_0 = 10$ for P (6 months) $= 0.4$ cm month^{-1}. Regardless of the initial condition, within a few months the solution is very close to the steady-periodic solution, and the final orbit is independent of the arbitrary initial condition. It is to be noted that maximum concentration occurs after the time of minimum precipitation; minimum concentration occurs at the time of maximum precipitation, and concentration remains low for some time afterward. Also, concentration is relatively high while precipitation rate is increasing, and relatively low while precipitation rate is decreasing. Physically, the results may be interpreted as follows: When the precipitation rate is small and concentration relatively small, the source term dominates and gradually builds up the concentration. As the precipitation rate begins to increase, concentration at first continues to increase because of the source, but continued increase of precipitation rate speeds up scavenging, and the concentration is eventually reduced. When the precipitation rate reaches a maximum, particulate matter is so efficiently scavenged that concentration reaches a minimum at the same time. As precipitation rate decreases after the maximum, scavenging is still important, and the source term only slowly increases the level of concentration. The clockwise orbit is produced in large part by the source during months of low precipitation. Other choices of parameters and precipitation variation lead to distortions of Fig. 12, but the clockwise sequence, the delay of maximum concentration until after minimum precipitation rate, and the pinching of the orbit near the time of maximum precipitation are characteristic of solutions to (10) in the case of a constant source.

It must be remarked, before looking at actual Sr-90 concentrations versus precipitation rate, that an orbital relationship between two out-of-phase cyclical variables is to be expected even in the absence of a physical relationship. For example, a plot of Sr-90 concentration in surface air versus temperature at Lima produces a clockwise sequence of points.

Figs. 13a–13d shows Sr-90 percent departures (from Fig. 2) versus precipitation rate at Miami, San Juan, Miraflores-Balboa, and percent departures in the latitude band 20–10°N versus worldwide average precipitation in the band. All curves resemble the solution to (10) shown in Fig. 12 to the extent that orbits are generally clockwise in time and maximum Sr-90 concentration occurs 1–4 months after minimum precipitation rate. Most curves show minimum concentration near the time of maximum precipitation rate. Three (Miami, San Juan and Balboa) show pinching together of the orbit and points near the

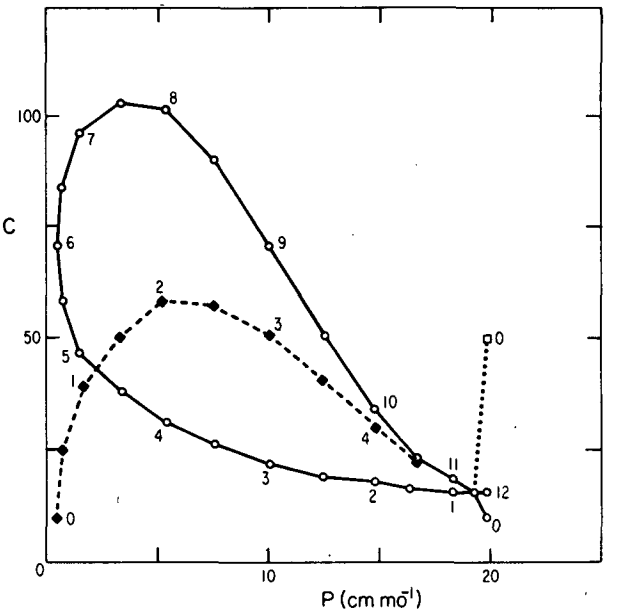

FIG. 12. Solution to (10) for S = constant = 30 month^{-1} $P(t) = 10 + 9.6\cos(2\pi t/12$ months) [cm month^{-1}], $k = 0.1$ cm^{-1} and (for initial conditions $C_0 = 10$ (solid), $C_0 = 50$ (dotted) when $P(0) = 19.6$ cm month^{-1}; and $C_0 = 10$ when P (6 months) $= 0.4$ cm month^{-1} (dashed). Numbers by points are times in months after initial condition [same as t in $P(t)$ in the first two cases, but time after P (6 months) $= 0.4$ cm month^{-1} in third case].

times of maximum precipitation. An interesting exception occurs in Fig. 13c, where the concentration increase from February to April is not accompanied by an increase in precipitation. A variable source is suggested. The solution to (10) shown in Fig. 12 was based on a smoothly varying precipitation rate and a constant source.

Figs. 14a–14d show percent departure versus precipitation at four stations of the sampling network along the 80th meridian in the Southern Hemisphere. Only the Guayaquil curve resembles the theoretical curve in Fig. 12 and the observations in the Northern Hemisphere shown in Fig. 13. At Lima and Santiago, the sequence of points is actually *counterclockwise.* However, precipitation rate at Lima is extremely low at all times (note scale), and is less than 0.13 cm month^{-1} during four months. This suggests that dry deposition may actually dominate during several months of the year, and (10) would not apply. The precipitation pattern at both Lima and Santiago, on the west coast of South America, is also not representative of zonal means, as shown by comparison of Figs. 15 and 16. Fig. 15 is a latitude-time section of precipitation rate using the stations of the 80th meridian radioactivity network with nearby substitutions (Kapuskasing for Moosonee and Puerto Aisen for Puerto Montt) where rainfall data were not readily available. Fig. 16 is a latitude-time section of precipitation rate constructed from zonal av-

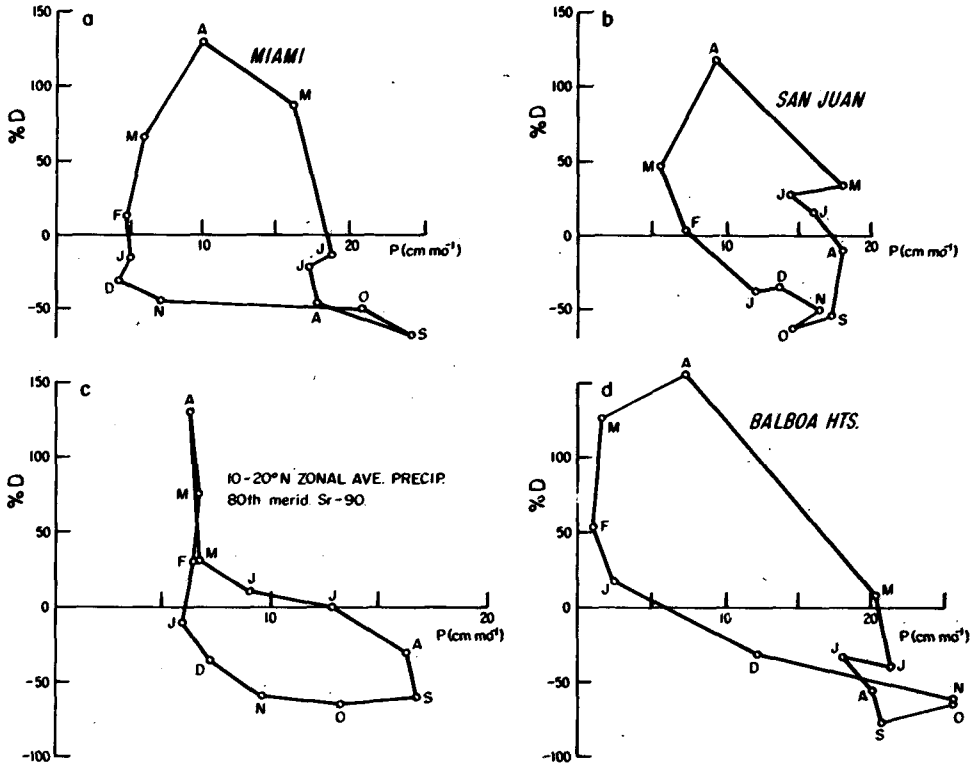

FIG. 13. Percentage departures of Sr-90 concentration in surface air as a function of precipitation rate during the course of a year for stations in the Northern Hemisphere. Precipitation record 30 years or more at Miami, San Juan and Balboa Heights.

erages over 10° latitude bands. The meridional migrations of the equatorial band of high precipitation rate is in phase with the migrations of the equatorial trough shown by Riehl (1979), which lag the sun by two months. The anomalous precipitation rate at Lima is obvious by comparison of Figs. 15 and 16.

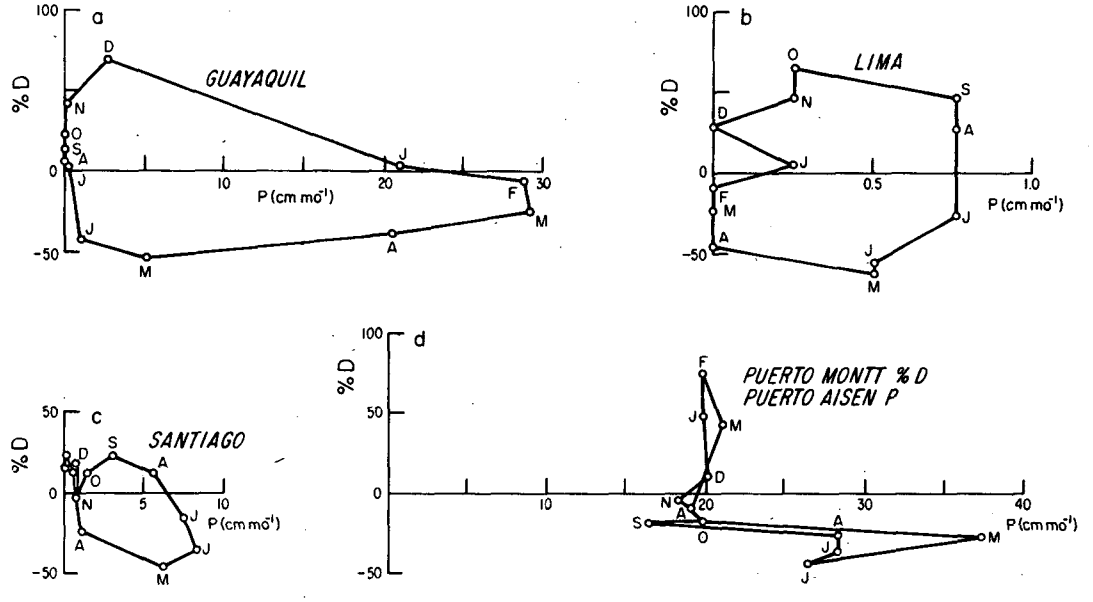

FIG. 14. As in Fig. 13 but for stations in the Southern Hemisphere. Precipitation record is 10 years at Guayaquil, 15 at Lima, 58 at Santiago, 11 at Puerto Aisen.

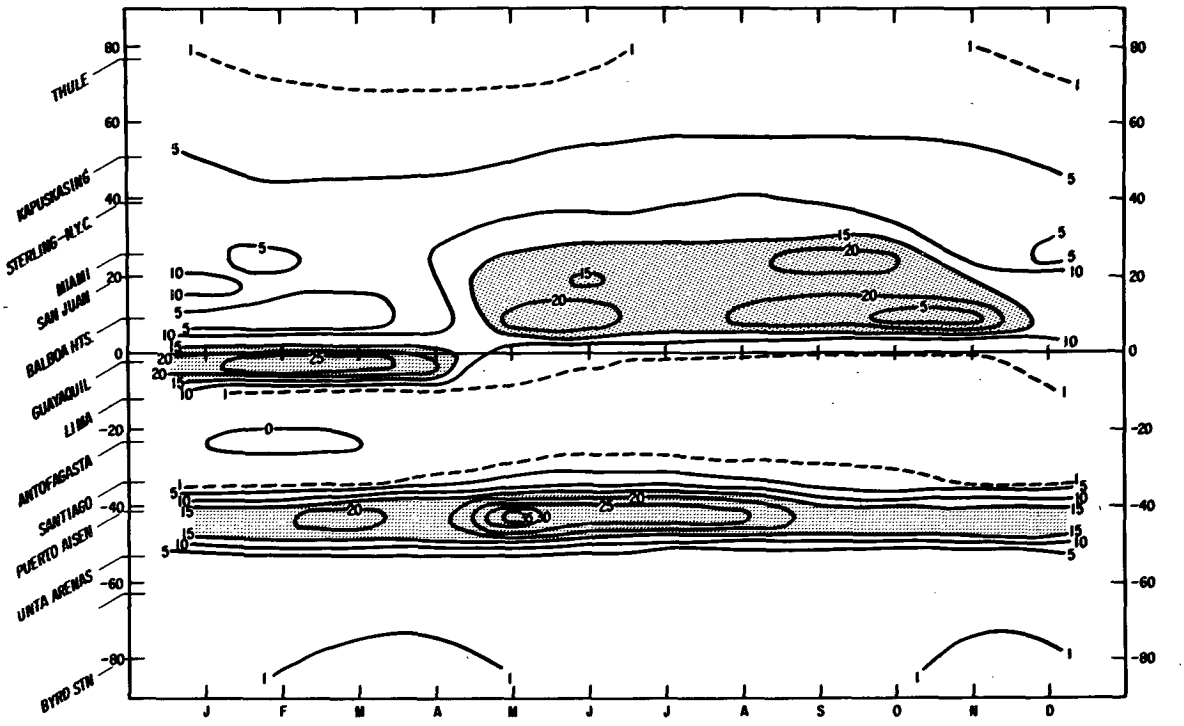

FIG. 15. Latitude-time section of precipitation rate (cm month^{-1}) at stations along the 80th meridian sampling network (Kapuskasing and Puerto Aisen substituted for Moosonee and Puerto Montt, respectively).

At Guayaquil and in the Northern Hemisphere, the 80th meridian precipitation rate is reasonably representative.

If the Lima Sr-90 percent deviations are plotted against zonal mean precipitation rate (from Fig. 15), a clockwise progression of points is obtained, although minimum concentration occurs three months after maximum precipitation rate. Maximum concentration occurs two months after minimum precipitation.

If the Santiago Sr-90 percent deviations are plotted against zonal mean precipitation rate, the point progression is still counterclockwise and similar to Fig. 14c, although the mean precipitation rate is much greater and deviations from the mean are smaller.

Fig. 14 shows Puerto Montt Sr-90 percent departures versus nearby Puerto Aisen precipitation rate. If zonal mean precipitation rate is used instead, the results are similar but smoother. The range of precipitation rate is smaller.

Comparison of Figs. 2 and 16 shows that, in the Northern Hemisphere, the first (second) half of the year is characterized by higher (lower) than average radioactivity and lower (higher) than average precipitation rate. In the Southern Hemisphere, the seasonal changes of radioactivity are more latitude-dependent, but so also is precipitation, and a negative correlation between radioactivity and precipitation rate occurs there also.

Figs. 2, 7, 13, 14, 15 and 16 confirm a relationship between precipitation rate and Sr-90 concentration in surface air. Where precipitation is zonally representative and not characterized by extremely small values allowing dry scavenging to dominate, the nature of the relationship is in the sense of the physical connection expressed by (10), which includes rain scavenging and a source (by transport). The relationship of Sr-90 to precipitation rate is most pronounced near the equator, where the seasonal variation of precipitation is large. At higher latitudes, radioactivity is not so closely tied to precipitation rate because the latter tends to show smaller seasonal variations and because of closer proximity to the seasonally varying stratospheric source. Nevertheless, seasonal variation of precipitation must be important wherever it occurs.

Hvinden *et al.* (1965) first recognized the important effect of precipitation rate on seasonal and latitudinal variations of radioactive fallout. They showed from a simple box model [having a term similar to that in (10) but allowing an exponentially decreasing source] that air concentration maxima and minima follow the minima and maxima, respectively, of precipitation rate. The lag was of the order of 2 months in an example. They were able to show a negative correlation between precipitation rate and Cs-137 activity in surface air using averages over seven Norwegian stations.

It is of interest to compare, in Fig. 17, the mean

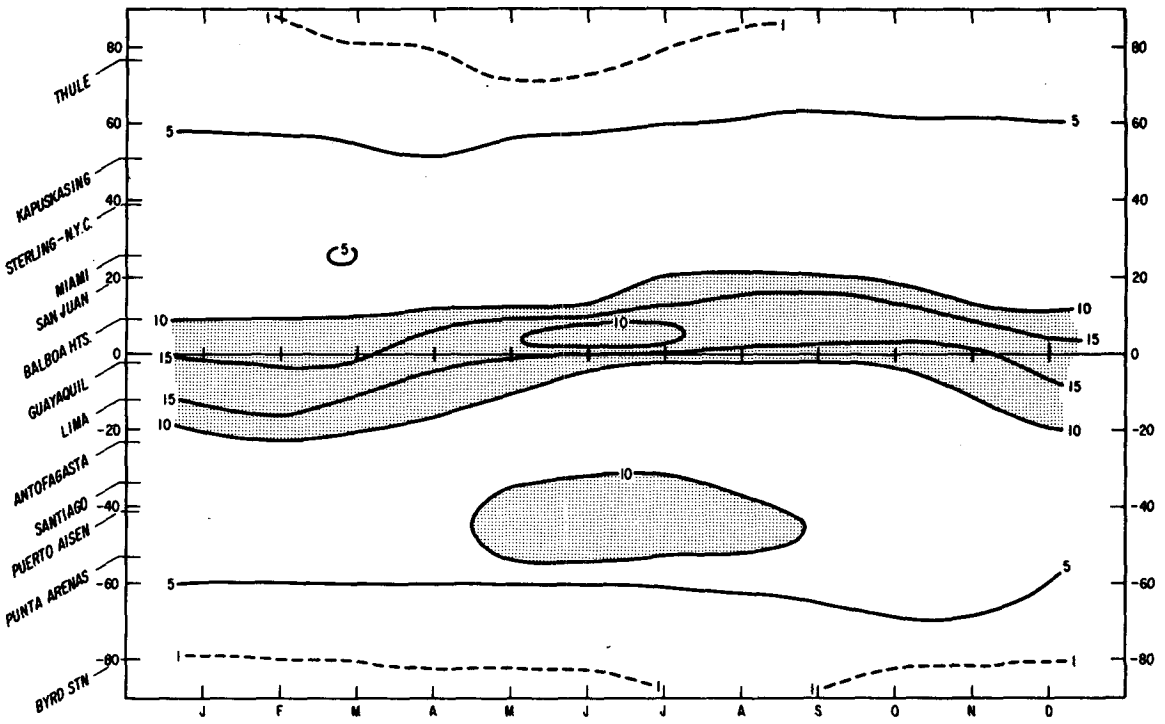

FIG. 16. Latitude-time sections of precipitation rate (cm month^{-1}) using zonal mean precipitation rates for 10° latitude bands.

latitudinal profile of Sr-90 concentration along the 80th meridian, as given by Table 1, with that of annual precipitation averaged zonally in 10° latitude bands. The minimum of Sr-90 near the equator corresponds to maximum precipitation. At 25°N and 25°S, the maximum of Sr-90 corresponds to a minimum of precipitation. At high latitudes, this inverse relationship is less consistent.

Fig. 17 further supports the importance of precipitation scavenging in producing observed concentrations, but does not show how precipitation and Sr-90 concentration interact to produce a maximum of scavenging away from the equator. Reference to (10) shows the Sr-90 scavenged over 12 mo is proportional to

$$\int_0^{12\text{ months}} CPdt \propto \sum_{12\text{ months}} CP.$$

Figs. 18a and 18b show this latter quantity computed from concentrations taken from Fig. 5 (80th meridian) and (a) P from 80th meridian data, and (b) zonally averaged precipitation. In 18a, the very low

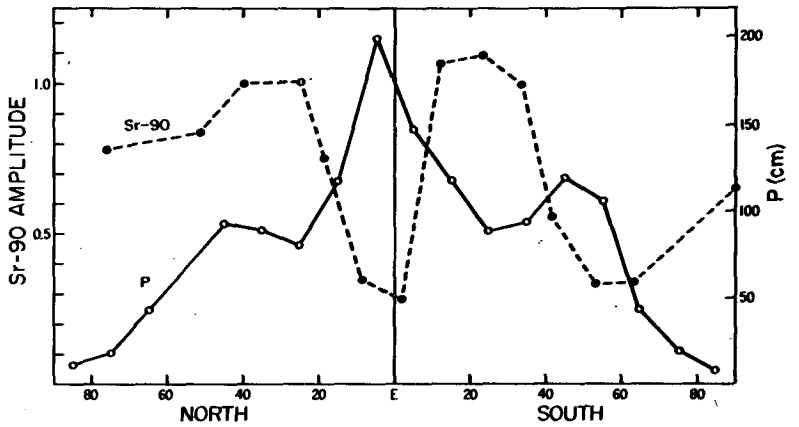

FIG. 17. Average amplitude profile of Sr-90 concentration in surface air (from Table 1) compared to profile of zonally averaged annual precipitation (from Fig. 16).

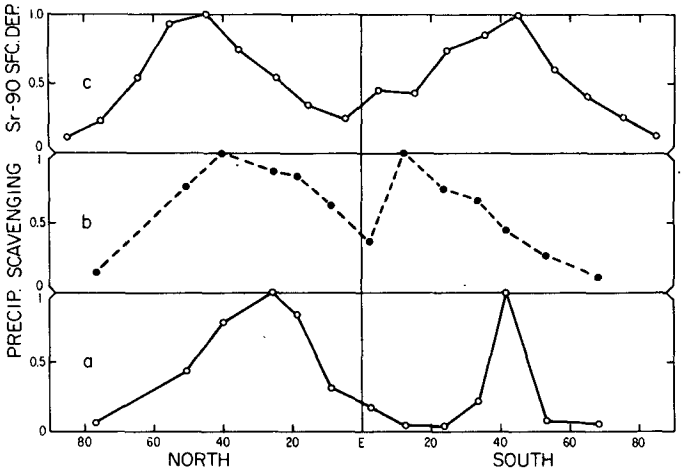

FIG. 18. Profiles of ΣCP, where C is mean Sr-90 concentration in surface air (from Fig. 5), P is precipitation rate, and the sum is over 12 months using (a) 80th meridian precipitation (Fig. 15) and (b) zonally averaged precipitation (Fig. 16). (c) Profile of cumulative Sr-90 deposits (per area) in 10° latitude bands at the end of 1979 (after Toonkel, 1980). All hemispheric maxima are arbitrarily set equal to unity.

precipitation rates along western South America produce little scavenging, and the maximum, essentially by default, occurs at Puerto Montt (41°27'S). In 18b, scavenging is large at these same latitudes. The Northern Hemisphere results are much more similar, although the latitudes of maximum scavenging are somewhat different. Fig. 18c shows the profile of cumulative Sr-90 deposits through 1979 at the earth's surface, based on worldwide measurements at land stations, as reported by Toonkel (1980). This updated deposit profile is very similar to one earlier reported by Hardy *et al.* (1968).

Because of its global basis, the profile in Fig. 18c is much smoother than the profiles in 18a and 18b. Aside from this difference, the maxima of deposition occur at higher latitudes than the maxima of surface-air scavenging. At least three possible reasons for this discrepancy suggest themselves: First, rain scavenging takes place throughout the troposphere, whereas the curves of 18a and 18b consider only scavenging of Sr-90 in surface air. Second, dry deposition contributes to 18c but not to 18a and 18b. Third, curves a and b are limited through concentration or precipitation, or both, to the 80th meridian. Certainly, 80th meridian precipitation is unrepresentative, and this probably contributes somewhat to making the Sr-90 concentration unrepresentative.

In view of the fact that radioactivity enters the troposphere from the stratosphere at high latitudes and subsequently descends equatorward, it seems likely that much will be scavenged at a higher latitude before it reaches the surface, thus leading to a deposition maximum poleward of the surface concentration maximum and the surface scavenging maximum.

9. Conclusion

The long time-series for Sr-90 concentration in surface air reveals a pronounced seasonality at all latitudes. Surprisingly, the spring maximum in the Northern Hemisphere appears first at the lowest latitude reporting (9°N) and appears later with increasing latitude up to 50°N, then appears earlier again. In the Southern Hemisphere, the spring maximum is not delayed with latitude and is found only equatorward of 40°S. It is replaced at higher latitudes by a broad late winter and spring minimum.

The delay of the spring maximum with increasing latitude within lower middle latitudes of the Northern Hemisphere was noted many years ago (Staley, 1963b) in a shorter record. This radioactivity pattern has now achieved much more statistical significance, and its similarity to the patterns of stratospheric mass change and northward jet-stream migration again suggests a physical connection.

The initial appearance of the Northern Hemisphere maximum at the lowest latitude seems to be largely the result of seasonal changes in precipitation scavenging associated with seasonal migration of the ITCZ. Seasonal precipitation scavenging is also important at low latitudes of the Southern Hemisphere and is probably important at all latitudes of both hemispheres, although obscured outside the tropics by seasonal variation of the stratospheric source.

Seasonal variations of Sr-90 in surface air along the extremely dry coast of western South America relate poorly to seasonal variations of local precipitation rate, but somewhat better to zonally averaged precipitation rate. However, insufficient Sr-90 measurements exist for other longitudes to conclude that

the Sr-90 measurements in the dry area are zonally representative.

The late summer Sr-90 maximum and late winter-spring minimum from middle to high southern latitudes have no apparent connection with either local or zonal mean precipitation rate. The seasonality of all climatological features is muted in the Southern Hemisphere, and there seems to be no obvious explanation for the seasonal variation of Sr-90 outside the equatorial rain belt. It is not known, however, to what extent the radioactivity variations at many southern latitudes are zonally representative.

The various features of the Sr-90 distribution in surface air, as well as the latitudinal distribution of zonally averaged surface deposition, represent for modelers an unsolved problem of atmospheric transport and scavenging. It would seem that tracer simulations should account more accurately for one or more of the following: sudden stratospheric warmings, tropopause formation, changes of stratospheric mass, thermal structure in the vicinity of the tropopause at high latitudes, transport from the lower stratosphere to the lower troposphere, and precipitation scavenging in the troposphere.

Acknowledgment. The author is indebted to W. D. Sellers for zonal average precipitation data.

REFERENCES

Danielsen, E. F., 1964: Report on Project Springfield. DASA 1517, Defense Atomic Support Agency, Washington, DC, 97 pp.

Dütsch, H. U., 1969: Atmospheric ozone and ultraviolet radiation. *World Survey of Climatology*, Vol. 4, *Climate of the Free Atmosphere*, D. F. Rex, Ed., Elsevier, 383–432.

Fabian, P., W. F. Libby and C. E. Palmer, 1968: Stratospheric residence time and interhemispheric mixing of strontium 90 from fallout in rain. *J. Geophys. Res.*, **73,** 3611–3616.

——, and P. G. Pruchniewicz, 1977: Meridional distribution of ozone in the troposphere and its seasonal variations. *J. Geophys. Res.*, **82,** 2063–2073.

Feely, H. W., H. Seitz, R. J. Largomarsino and P. E. Biscaye, 1966: Transport and fallout of stratospheric radioactive debris. *Tellus*, **18,** 316–328.

——, L. E. Toonkel and R. J. Larsen, 1980: Radionuclides and trace metals in surface air. Environmental Quarterly, Environmental Measurements Laboratory, Department of Energy, EML-381 (Appendix), Part C, 1–193.[2]

Gustafson, P. F., 1961: Measurement of air-borne radioactivity by gamma-ray scintillation spectrometry. *Proc. Upper Atmosphere Sampling Symposium*, Part I, Albuquerque, Sandia Corporation (SCR-420), 113–129.[2]

Hardy, E. P., M. W. Meyer, J. S. Allen and L. T. Alexander, 1968: Strontium-90 on the earth's surface. *Nature*, **219,** 584–587.

Hvinden, T., A. Lillegraven and O. Lillesaeter, 1965: Precipitation as a cause of seasonal and latitudinal variations in radioactive fallout. *Nature*, **206,** 461–463.

Junge, C. E., 1963: *Air Chemistry and Radioactivity*. Academic Press, 382 pp.

Kida, H., 1977a: A numerical investigation of the atmospheric general circulation and stratospheric tropospheric mass exchange. I. Long-term integration of a simplified general circulation model. *J. Meteor. Soc. Japan*, **55,** 52–70.

——, 1977b: A numerical investigation of the atmospheric general circulation and stratospheric tropospheric mass exchange. II. Lagrangian motion of the atmosphere. *J. Meteor. Soc. Japan*, **55,** 71–88.

Krey, P. W., and B. T. Krajewsky, 1972: Updating stratospheric inventories to July 1971. Quarterly Summary Rep., Health and Safety Laboratory, U.S. Atomic Energy Commission, HASL-257, Part I, 33–50.[2]

Leifer, R., M. Schonberg and L. Toonkel, 1976: Updating stratospheric inventories to July 1975. Environmental Quarterly, Health and Safety Laboratory, Energy Research and Development Administration, HASL-306, Part I, 127–142.[2]

——, R. Larsen and L. Toonkel, 1979: Updating stratospheric inventories to July 1978. Environmental Quarterly, Environmental Measurements Laboratory, Department of Energy, EML-363, Part I, 109–124.[2]

Libby, W. F., 1956: Radioactive strontium fallout. *Proc. Natl. Acad. Sci., U.S.A.*, **42,** 365–390.

Lockhart, L. B., R. A. Baus, R. L. Patterson and A. W. Saunders, 1960: Radiochemical analyses of fission debris in the air along the 80th meridian west. *J. Geophys. Res.*, **65,** 1711–1722.

Machta, L., 1957: The nature of radioactive fallout and its effect on man. Hearings Before the Special Subcommittee on Radiation of the Joint Committee on Atomic Energy, 27 May–7 June, 1957, Parts 1 and 2. [U.S. Government Printing Office].

——, and K. Telegadas, 1973: Examples of stratospheric transport. *Proc. Second Conf. Climatic Impact Assessment Program*, A. J. Broderick, Ed., 47–56. [DOT-TSC-OST-73-4].

Mahlman, J. D., and W. J. Moxim, 1978: Tracer simulation using a global general circulation model: Results from a midlatitude instantaneous source experiment. *J. Atmos. Sci.*, **35,** 1340–1374.

Martell, E. A., 1959: Atmospheric aspects of Strontium-90 fallout. *Science*, **129,** 1197–1206.

——, and H. E. Moore, 1974: Tropospheric aerosol residence times: A critical review. *J. Rech. Atmos.*, **8,** 903–910.

Reed, 1955: A study of a characteristic type of upper-level frontogenesis. *J. Meteor.*, **12,** 226–237.

——, and F. Sanders, 1953: An investigation of the development of a mid-tropospheric frontal zone and its associated vorticity field. *J. Meteor.*, **10,** 338–349.

Reiter, E., 1963: A case study of meteorological fallout. *J. Appl. Meteor.*, **2,** 691–705.

Riehl, H., 1979: *Climate and Weather in the Tropics*. Academic Press, 611 pp.

Staley, D. O., 1960: Evaluation of potential-vorticity changes near the tropopause and the related vertical motions, vertical advection of vorticity, and transfer of radioactive debris from stratosphere to troposphere. *J. Meteor.*, **17,** 591–620.

——, 1962: On the mechanism of mass and radioactivity transport from stratosphere to troposphere. *J. Atmos. Sci.*, **19,** 450–467.

——, 1963a: Stratospheric mass variations and fission product radioactivity in surface air. *J. Atmos. Sci.*, **20,** 615–621.

——, 1963b: Atmospheric circulation from fission-product radioactivity in surface air. *Science*, **140,** 667–670.

Toonkel, L., 1980: Worldwide deposition of Sr-90 through 1979. Environmental Quarterly, Environmental Measurements Laboratory, Department of Energy, EML-381, Part I, 153–165.[2]

[2] Available from NTIS, U.S. Dept. Commerce, 5285 Port Royal Rd., Springfield, VA 22161.